Hybrid Single-Line-to-Ground Fault Arc Suppression Method in Distribution Networks

Qiong Liu(✉), Wen Wang, Qinze Chen, Chaofeng Zhang, and Xiao Ding

Changsha University of Science and Technology, Changsha, China
1424623598@qq.com

Abstract. Existing voltage-type arc suppression method compensates fault current without considering line impedance. When metallic single line-to-ground (SLG) fault occurs, residual current of fault location rises instead of falling with conventional method, resulting in the failure of arc suppression. To solve this problem, combined current-type and voltage-type arc suppression method, a hybrid method is proposed in this paper. The distribution network is analyzed when considering line impedance and load. According to this, the current and voltage references for active arc suppression device (ASD) are derived for accurate arc suppression. The grounding resistance is estimated by zero-sequence current and voltage of the system. When it is larger than a setting threshold, voltage-type arc suppression method is adopted. Otherwise, current-type method is adopted. The proposed method can reduce fault current to almost zero. The correctness of the proposed method is validated and comparison is presented by simulation in the MATLAB/Simulink environment.

Keywords: Distribution Network · Single-phase-to-ground Fault · Arc Suppression

1 Introduction

SLG (single line-to-ground) faults are the most common fault type and shound be paid attention to [1, 2]. With the the extensive use of power cables, the fault current increases sharply. The resulted ground-fault arc is difficult to extinguish itself, which may cause overvoltage and interphase short circuit [3, 4].

The passive method adopts Petersen coil to acchive capacitive current compensation [5–7]. The active method uses power electronics converters to inject a specific zero-sequence current for full ground-fault current compensation. Z. Zheng [8] presented a three-phase arc suppression device and backstepping control. However, the accuracy of the ground-fault current limits its arc suppression performance. The conventional method [4] achieve arc suppression by setting neutral voltage to the inverse of supply voltage of faulty phase.

However, line impedance is ignored. To address this problem, [9, 10] proposed an arc suppression method by limiting the neutral voltage to a regulated reference. The effect

H. Yang et al. (Eds.): SmartGIFT 2022, LNICST 483, pp. 371–385, 2023.
https://doi.org/10.1007/978-3-031-31733-0_31

of line impedance and load are taken into account [10]. However, the simulation was performed when grounding resistance is set to 30,50 and 100Ω. It ignores the conditions of low grounding resistance and metallic SLG faults. When low-resistance SLG fault occurs at the beginning of faulty feeder, the actual value of neutral voltage is close to the reference, which may leads to the failure of arc suppression.

In this paper, a hybrid method is proposed in Sect. 2. In Sect. 3, the limitations of conventional method and the impact factors of residual current are analyzed. Then, the injection current reference and neutral voltage reference are presented along with the related parameters calculation. The complete implementation process of the hybrid arc suppression method is presented. Finally, simulation results are provided in Sect. 4 to study arc suppression performance.

2 Performance Analysis of Conventional Arc Suppression Method

Conventional arc suppression method works by regulating the neutral voltage to the supply voltage of faulty phase. However, conventional arc suppression method ignores line impedance and load, which leads to an issue that the voltage of fault location is the same as bus. The residual voltage cannot be restricted to zero even bus voltage maintains zero.

2.1 Residual Current Calculation at Fault Location

Figure 1 shows a 10kV distribution network including line impedance and load. The feeder lines length is m km long and the fault feeder is l km long. α is the fault location ratio, i.e., the division of the length from the busbar to the fault point over the total length of the fault feeder. Z_{lX} and Z_{load} are the line impedance and load impedance, respectively. The load is in triangular connection.

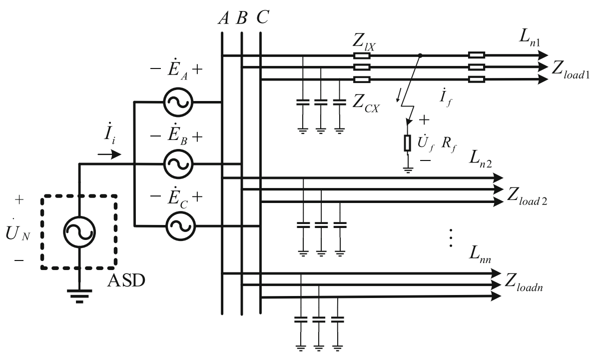

Fig. 1. 10kV distribution network considering line impedance.

The boundary conditions is

$$\begin{cases} \dot{U}_{f1} + \dot{U}_{f2} + \dot{U}_{f0} = \dot{U}_f \\ \dot{I}_{f1} = \dot{I}_{f2} = \dot{I}_{f0} = \frac{1}{3}\dot{I}_f \end{cases} \tag{1}$$

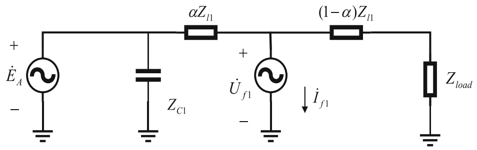

(a) Positive-sequence network.

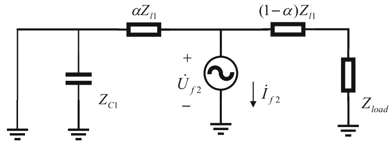

(b) Negative-sequence network.

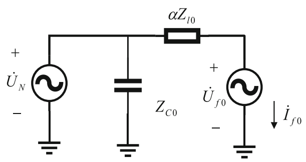

(c) Zero-sequence network.

Fig. 2. The sequence networks considering line impedance.

From (1) and Fig. 2, the simplified circuit is shown as Fig. 3, where $Z_{LD} = Z_{load} + (1 - \alpha)Z_{l1}$.

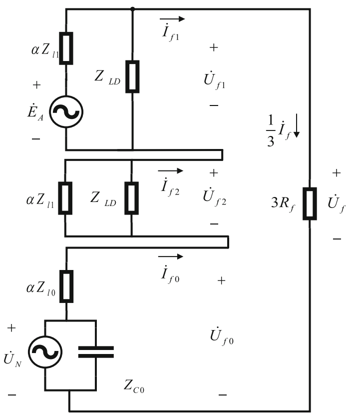

Fig. 3. The simplified composite sequence network.

$\dot{E}_{eq}$ and Z_{eq} are the equivalent voltage source and impedance, shown as (2) and (3).

$$\dot{E}_{eq} = \frac{Z_{load}+(1-\alpha)Z_{l1}}{Z_{l1}+Z_{load}}\dot{E}_A + \dot{U}_N \tag{2}$$

$$Z_{eq} = \frac{2\alpha Z_{l1}[Z_{load}+(1-\alpha)Z_{l1}]}{Z_{l1}+Z_{load}} + \alpha Z_{l0} \tag{3}$$

Therefore, the ground-fault current $\dot{I}_f$ is

$$\dot{I}_f = \frac{3\dot{E}_{eq}}{Z_{eq}+3R_f} \tag{4}$$

Assume $\dot{I}_f$ is equal to zero, from (2) - (4), we can get the reference neutral voltage of the ASD for ground-fault arc suppression, which is shown in (5).

$$\dot{U}_N^* = -\frac{Z_{load}+(1-\alpha)Z_{l1}}{Z_{l1}+Z_{load}}\dot{E}_A \tag{5}$$

According to (1) and (2)-(4), the residual current with conventional voltage-type arc suppression method can be obtained by (6).

$$\dot{I}_{r0} = \frac{-3\alpha Z_{l1}\dot{E}_A}{(\alpha Z_{l0}+3R_f)(Z_{l1}+Z_{load})+2\alpha Z_{l1}[Z_{load}+(1-\alpha)Z_{l1}]} \tag{6}$$

Obviously, the residual current mainly relates to α, R_f and Z_{load}. Typical power system parameters are shown in Table 1.

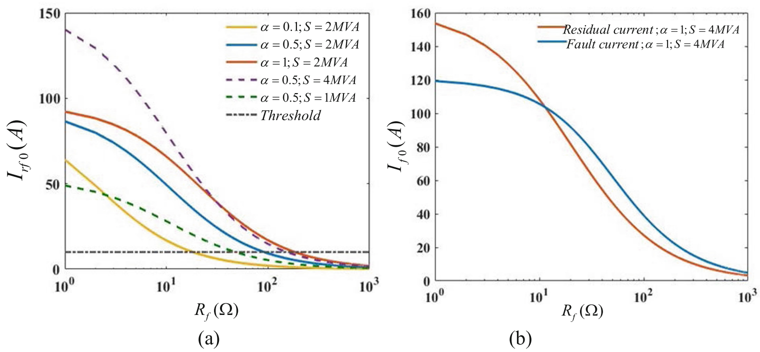

Fig. 4. The residual currents when parameters vary (a) and comparison fault current before and after conventional arc suppression (b).

According to (6), the relationship between fault location, grounding resistance and residual currents are shown in Fig. 4(a). From the operation code, the maximum residual current to ensure fault arc self-extinction is 10 A, which is set as the threshold in Fig. 4(a).

It is shown that when the load power is fixed, the residual current increases as the fault gets close to the end of the fault feeder. It can be also observed that with the decrease of grounding resistance, the residual current increases. Only when the grounding resistance is larger than about 200 Ω, the arc can be suppressed.

Figure 4(b) shows the comparison fault currents before and after conventional arc suppression when $\alpha = 1$ and $S = 4MVA$. The red curve is the residual current after arc suppression. The blue curve is the fault current before arc suppression. We can see that the residual current is even larger than the fault current before SLG fault. In the worst case, the fault current reaches 130% of the capacitive current when grounding resistance is zero.

Table 1. System parameters.

Parameters	Value
Positive-sequence impedances Z_{l1}	0.27 + j0.07 Ω/km
Positive-sequence impedances Z_{c1}	9.4e3 Ω/km
Zero-sequence impedances Z_{l0}	2.7 + j0.32 Ω/km
Zero-sequence impedances Z_{c0}	1.14e4 Ω/km
Nominal power	1 MVA
Line voltage E_X	10 kV
Total length of feeder lines m	100 km
Total length of fault line l	20 km

3 Hybrid Arc Suppression Method

Current-type arc suppression method needs the distributed parameters. Their detection may be affected by the fluctuation and asymmetry of the distribution network. These factors will lead to measurement errors of grounding parameters, so that the reference injected current is not accurate enough, and it is difficult to restrict fault current to zero. Voltage-type method needs no measurement of grounding parameters, but it has poor performance when low resistance SLG fault occurs. To solve this problem, a hybrid arc suppression method is proposed.

3.1 Principle of Hybrid Arc Suppression Method

The proposed method is shown as follows. When the estimated grounding resistance is larger than a set threshold, voltage-type arc suppression method is adopted. Otherwise, the current-type method will be adopted. Through the complementary advantages of the two methods, the arc suppression performance is maximized.

According to (6), the critical resistance of voltage-type arc suppression failure R_{cr} can be obtained from (7).

$$R_{cr} = \left| \frac{0.3Z_{l1}\dot{E}_A - 20\alpha Z_{l1}[Z_{load} + (1-\alpha)Z_{l1}]}{30(Z_{l1} + Z_{load})} - \frac{\alpha Z_{l0}}{3} \right| \tag{7}$$

Thus, the switching conditions of voltage-type and current-type arc suppression methods are as follow:

1) When $R_f \geqslant R_{cr}$, voltage-type arc suppression method is adopted.
2) When $R_f < R_{cr}$, current-type arc suppression method is adopted.

3.2 Neutral Voltage and Injected Current for Arc Suppression

From circuit theory, the composite sequence network considering the line impedance, fault location and the load impedance can be deduced from Fig. 3 as shown in

Fig. 5, where Z_a is the equivalent impedance, i.e., $Z_a = \alpha Z_{l1}//Z_{LD} = \alpha Z_{l1}[Z_{load} + (1-\alpha)Z_{l1}]/(Z_{l1} + Z_{load})$.

If the current-type ASD is used, the equivalent voltage source and impedance can be obtained from Fig. 5(a), as shown in (8) and (9).

$$\dot{E}_{eq} = \frac{Z_{load}+(1-\alpha)Z_{l1}}{Z_{l1}+Z_{load}}\dot{E}_A + \frac{Z_{C0}\dot{I}_i}{3} \tag{8}$$

$$Z_{eq} = \frac{2\alpha Z_{l1}[Z_{load} + (1-\alpha)Z_{l1}]}{Z_{l1} + Z_{load}} + \alpha Z_{l0} + Z_{C0} \tag{9}$$

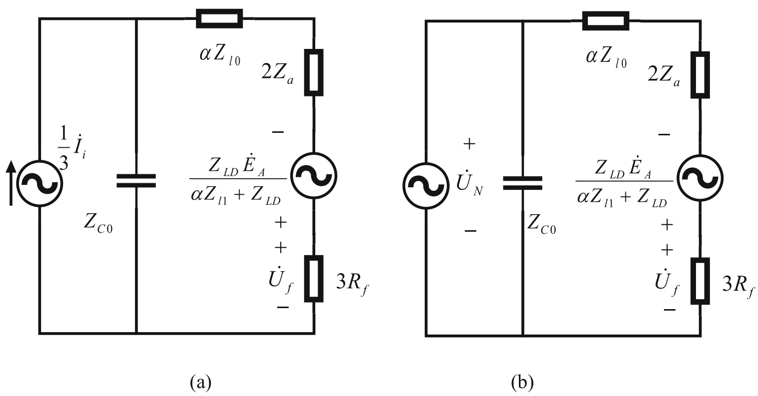

Fig. 5. Simplified composite sequence network when the line impedance is considered (a: with current-type ASD; b: with voltage-type ASD).

Assume $\dot{I}_f$ is equal to zero, from (8) and (9), we can get the reference injected current of the ASD for arc suppression,

$$\dot{I}_i^* = -\frac{3[Z_{load}+(1-\alpha)Z_{l1}]}{(Z_{l1}+Z_{load})Z_{C0}}\dot{E}_A \tag{10}$$

If the reference current $\dot{I}_i^*$ is injected to the neutral, the ground fault current can be restricted to zero. Take notice that (10) is related to fault location, line impedance, load impedance and phase-to-ground impedance. Both of fault location and load impedance need to be measured in real-time, and the distributed capacitance should be estimated in advance.

For the voltage-type ASD, the reference neutral voltage of the ASD can be deduced by setting $\dot{U}_f = 0$ in Fig. 5(b),

$$\dot{U}_N^* = -\frac{Z_{load}+(1-\alpha)Z_{l1}}{Z_{l1}+Z_{load}}\dot{E}_A \tag{11}$$

Voltage-type arc suppression method brings the advantage that it needs no measurement distributed parameters of the feeder line. To implement the proposed method, the grounding resistance should be know.

Assume Y_X is the phase-to-ground admittance. $\dot{I}_0$ is the zero-sequence current of after SLG fault, which can be expressed as (12)

$$\dot{I}_0 = \dot{U}_0\left(Y_A + Y_B + Y_C + \frac{1}{R_f}\right) \tag{12}$$

where $\dot{U}_0$ is the zero-sequence voltage. The expression of ground-fault resistance is as follow:

$$R_f = \frac{\dot{U}_0}{\dot{I}_0 - \dot{U}_0(Y_A + Y_B + Y_C)} \tag{13}$$

There are many methods for fault location [14]–[17], it is not discussed in this paper.

The load impedance to the distribution network transformer is equivalent to Y-type impedance Z_{load}. It is assumed that load current is basically unchanged before and after the fault. During normal operation, the load impedance meets (14).

$$\dot{E}_A\left(\frac{\dot{E}_A}{Z_{load}}\right)^* = \frac{P_L + jQ_L}{3} \tag{14}$$

where P_L and Q_L are the active and reactive power of fault feeder, respectively. Thus the expression of Z_{load} is (15).

$$Z_{load} = \frac{3E_A^2}{P_L - jQ_L} \tag{15}$$

Therefore, the injection current reference and neutral voltage reference can be expressed as follows, respectively, according to (9), (10) and (15).

$$\dot{I}_{ref} = 3\left[\frac{\alpha Z_{l1}(P_L - jQ_L)}{3\left|\dot{E}_A\right|^2 + Z_{l1}(P_L - jQ_L)} - 1\right]\frac{\dot{E}_A}{Z_{C0}} \tag{16}$$

$$\dot{U}_{ref} = \left[\frac{\alpha Z_{l1}(P_L - jQ_L)}{3\left|\dot{E}_A\right|^2 + Z_{l1}(P_L - jQ_L)} - 1\right]\dot{E}_A \tag{17}$$

3.3 Implementation

Figure 6 shows the implementation of the proposed method. When SLG fault occurs. The fault phase and feeder will be identified immediately. The grounding resistance, load impedance and fault location can be calculated according to (13), (15), respectively. If $R_f \geqslant R_{cr}$, the voltage-type method is chosen and the ASD controls the neutral voltage to the reference value according to (17). Otherwise, the current-type method is chosen to inject reference current to the neutral point according to (16).

After a delay, we reduce the injected current and judge whether the zero-sequence voltage changes in proportion to make sure the fault status. When the neutral voltage decreases with the decrease of injection current, it means the fault disappears and remove the injected current. Otherwise, it will be judged as permanent fault and line selection and protection device should be triggered.

3.4 Arc Suppression Accuracy of the Proposed Hybrid Method

By controlling the injected current as (9) or neutral voltage as (10), the residual current can be reduced to zero. According to (9) and (10), the fault location must be known in advance. However, the fault location is very difficult to measure accurately. It is necessary to further analyze the residual current when estimated fault location varies.

It is assumed that the estimated fault location ratio is α_{es}. The existing fault location method can limit $|\alpha_{es} - \alpha|$ to less than 10%. According to (7)-(9), the residual current with current-type arc suppression method can be obtained from (17).

$$\dot{I}_{rc} = \frac{3(\alpha_{es} - \alpha)Z_{l1}\dot{E}_A}{(\alpha Z_{l0} + Z_{C0} + 3R_f)(Z_{l1} + Z_{load}) + 2\alpha Z_{l1}[Z_{load} + (1-\alpha)Z_{l1}]} \quad (18)$$

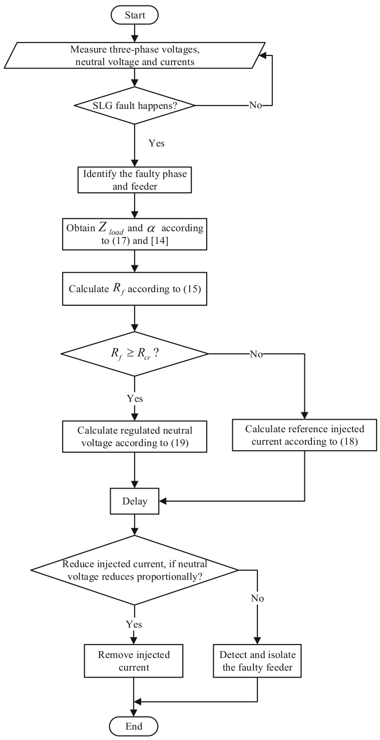

Fig. 6. Implementation of proposed hybrid arc suppression method.

Set $|\alpha_{es} - \alpha| = 10\%$, the relationships between fault location, grounding resistance and residual current with proposed current-type arc suppression are shown in Fig. 7. The residual current decreases with the increase of grounding resistance. With the proposed current-type arc suppression method, the residual current can be limited to a low value within 7A, which has better performance than conventional method.

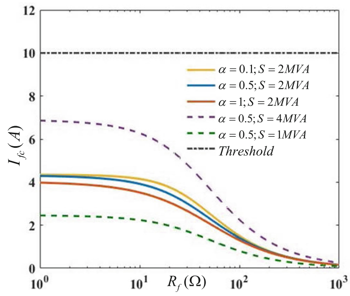

Fig. 7. The residual current with proposed current-type arc suppression.

According to (10) and Fig. 6(b), the residual current with voltage arc suppression method is shown as (19).

$$\dot{I}_{rv} = \frac{3(\alpha_{es} - \alpha)Z_{l1}\dot{E}_A}{(\alpha Z_{l0} + 3R_f)(Z_{l1} + Z_{load}) + 2\alpha Z_{l1}[Z_{load} + (1-\alpha)Z_{l1}]} \tag{19}$$

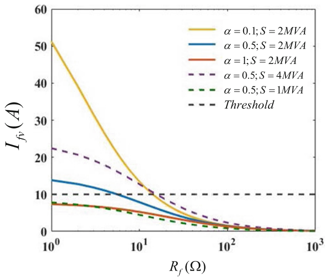

Fig. 8. The residual current with proposed voltage-type arc suppression.

When the proposed method is adopted, the relationships between fault location, grounding resistance and residual current are shown in Fig. 8. With the decrease of grounding resistance and α, the residual current increase. When grounding resistance is low, the residual current is over 10A and arc suppression fails. The failure in case of low resistance SLG fault with voltage-type method should be considered (Fig. 9).

4 Simulation Results

MATLAB/Simulink is used to testify the arc suppression performance of hybrid method and conventional method. A $10kV$ distribution network is built, as shown in Fig. 10. C1, C2 and C3 are cables, the other feeders are overhead lines with the parameters in Table 2. In the simulation, the SLG fault occurs at phase A. K1, K2, K3 and K4 are the fault locations. The error of fault location method is assumed as 10%. The comparative performance waveforms with conventional and proposed method under different α, R_f and Z_{load} are as shown in Figs. 10, 11, 12 and 13.

The arc suppression rate η is used, which is defined by

$$\eta = 1 - \frac{I_r}{I_f} \tag{20}$$

Table 2. Line parameters.

Types	Positive-sequence parameters			Zero-sequence parameters		
	$R_1\ \Omega/km$	$L_1\ (mH/km)$	$C_1\ (\mu F/km)$	$R_1\ \Omega/km$	$L_1\ (mH/km)$	$C_1\ (\mu F/km)$
Overhead line	0.17	1.21	0.011	0.23	5.48	0.008
Cable	0.27	0.255	0.339	2.7	1.019	0.28

Table 3. Simulation results for Arc suppression methods in different grounding resistance.

Fault location	R_f (Ω)	I_f (A)	Conventional method		Proposed voltage-type method		Proposed current-type method	
			Fault residual current I_r (A)	$\eta(\%)$	Fault residual current I_r(A)	$\eta(\%)$	Fault residual current I_r (A)	$\eta(\%)$
K3	0 ($R_f < R_{cr}$)	85.1	150.8	−77.2			3.9	95.4
K3	27 ($R_f = R_{cr}$)	78.3	43.1	45.0	10.2	87.0	3.6	95.4
K3	100 ($R_f > R_{cr}$)	50.8	14.7	71.1	3.7	92.7		

Table 4. Simulation results for Arc suppression methods in different load.

Fault location	R_f (Ω)	I_{load} (A)	I_f (A)	Conventional method		Proposed method	
				Fault residual current I_r (A)	$\eta(\%)$	Fault residual current I_r (A)	$\eta(\%)$
K2	100	112.5	46.7	5.79	87.6	2.0	95.7
K3	100	248.4	50.8	14.7	71.1	3.7	92.7

Table 5. Simulation results for Arc suppression methods in different fault location.

Fault location	R_f (Ω)	I_f (A)	Conventional method		Proposed method	
			Fault residual current I_r (A)	$\eta(\%)$	Fault residual current I_r (A)	$\eta(\%)$
K1	100	54.1	12.2	77.4	4.5	91.7
K3	100	50.8	14.7	71.1	3.7	92.7
K4	100	40.4	23.8	41.1	3.9	90.3

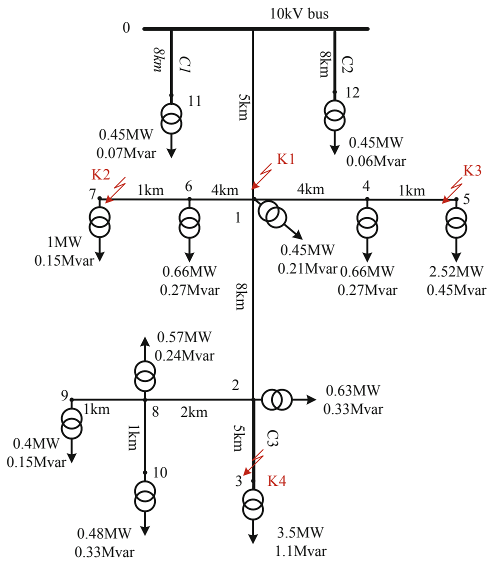

Fig. 9. Modified IEEE 13-node test system.

4.1 Case 1

To compare the arc suppression performance in different grounding resistance, the fault location is set at K3 with the grounding resistances 0Ω, 27Ω and 100Ω. When SLG fault occurs at K3, R_{cr} is 27Ω which is calculated by (13). The comparative fault current waveforms are shown in Fig. 10 and the simulation results are shown in Table 3.

As shown in Fig. 10(a), when metallic SLG fault occurs, the fault current after conventional arc suppression is even larger than before, which has no arc suppression performance. When grounding resistance increases, the fault current will decrease. When the fault location is K3 and R_f is 100Ω, the fault current is 14.7A, which is higher than the threshold 10A and is affected by grounding resistance.

However, proposed method can reduce the residual current to a lower value and is not affected by grounding resistance. When metallic SLG fault occurs, the arc suppression rate is 95.4%.

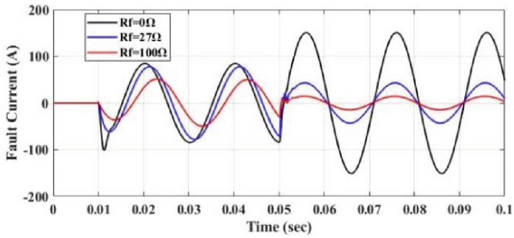

(a) Fault current waveforms adopting the conventional method when R_f varies.

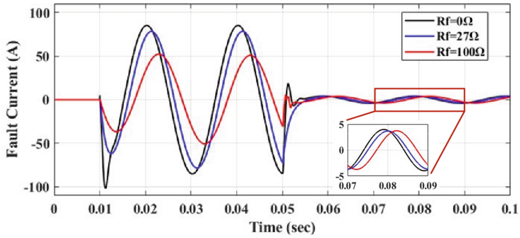

(b) Fault current waveforms adopting the proposed method when R_f varies.

Fig. 10. Comparative fault current waveforms adopting the proposed method and the conventional one when R_f varies.

To explain the influence of grounding resistance for proposed arc suppression method, R_f is set as $R_{cr} = 27\Omega$, the comparative curves are shown in Fig. 11. Obviously, when low resistance SLG fault occurs, the fault current can be reduced to 3.6A with current-type method. However, when voltage-type method is adopted, the fault current is over 10A, which will lead to arc suppression failure. This is mainly because voltage-type arc suppression has its dead zone. That is to say, when the grounding resistance is lower than R_{cr}, voltage-type method fails. It is also consistent with the previous analysis. When the detected grounding resistance is smaller than R_{cr}, the current-type arc suppression strategy is adopted in proposed hybrid method. The proposed hybrid method can solve this problem.

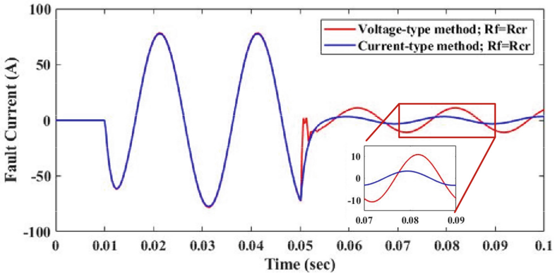

Fig. 11. Comparative fault current waveforms adopting the proposed voltage-type and current-type methods.

4.2 Case 2

The performance comparison of different load is performed, and the comparative waveforms are shown in Fig. 12 and the simulation results are shown in Table 4. It is obvious that conventional method has a large residual current, which may lead to the failure of arc suppression and is affected by load. Moreover, according to the black curve and blue curve, with the increase of load power, the residual current with conventional method will increase too. This is mainly because the line impedance and load impedance are parallel and when load impedance is smaller, the influence of line impedance is relatively obvious. We can also see that proposed method always performs better than conventional method, the residual current is < 4A.

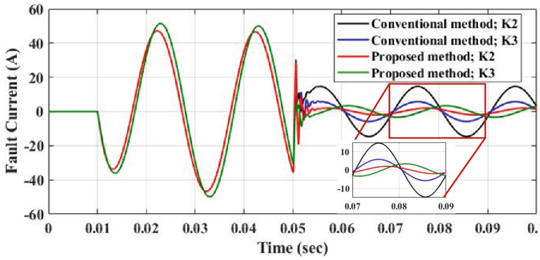

Fig. 12. Comparative fault current waveforms adopting the proposed voltage-type and current-type meth-ods when load varies.

4.3 Case 3

Figure 16 shows the comparative waveforms adopting the proposed method and conventional method when fault distance varies. Table 5 shows the simulation dates. K1 is close to the busbar. K3 is adjacent to the end of fault feeder. According to Fig. 13(a), conventional method can hardly reduce fault current less than 10A. We can see that the residual current at K3 is higher than at K1. This is mainly because when α is small, the series inductive line impedance partly compensates the phase-to-ground capacitance.

Figure 13(b) indicates that the residual currents of proposed method are < 5A and is not influenced by fault location. In addition, when SLG fault occurs at K4, the fault feeder is a mixture of overhead lines and cables. The proposed method still works, and which is also not affected by line structure.

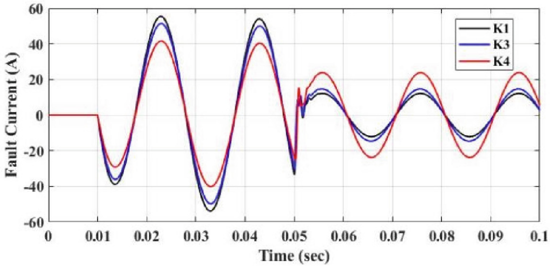

(a) Fault current waveforms adopting the conventional method when fault distance varies.

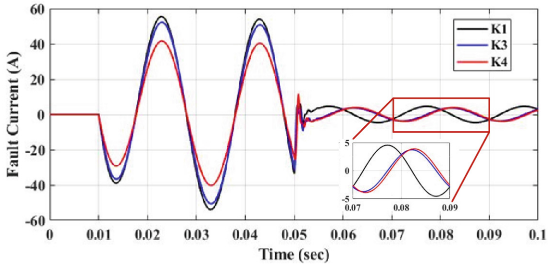

(b) Fault current waveforms adopting the proposed method when fault distance varies.

Fig. 13. Comparative fault current waveforms when fault distance varies.

5 Conclusions

The conventional voltage-type arc suppression method cannot effectively extinguish arc especially when low resistance SLG fault occurs. To solve the issue, this paper proposes a hybrid arc suppression method. Combine with voltage-type method, which need no measurement grounding parameters, and a current-type method, which is effective for low resistance SLG fault, and the residual current can be almost restricted to zero. Compare to conventional method, the proposed ones can effectively achieve arc suppression rate over 90% in spite of influence of line impedances, grounding resistances and loads.

References

1. Burgess, R.: Minimising the risk of cross-country faults in systems using arc suppression coils. Iet Generation Transmission & Distribution **5**(7), 703–711 (2011)
2. Vaziri, M.: Grounding of primary system for LV networks. IEEE Transactions on Power Delivery **31**(2), 419–427 (2016)
3. Guo, M.: Deep-learning-based earth fault detection using continuous wavelet transform and convolutional neural network in resonant grounding distribution systems. IEEE Sensors Journal (2017)
4. Wang, W.: Principle and design of a single-phase inverter-based grounding system for neutral-to-ground voltage compensation in distribution networks. IEEE Transactions on Industrial Electronics **64**(2), 1204–1213 (2017)
5. Ouyang, S.: Control strategy for Arc-suppression-coil-grounded star-connected power electronic transformers. IEEE Transactions on Power Electronics **6**(34), 5294–5311 (2019)

6. Brenna, M.: Petersen coil regulators analysis using a real-time digital simulator. IEEE Transactions on Power Delivery **26**(3), 1479–1488 (2011)
7. Zeng, X.: Some novel techniques for insulation parameters measurement and petersen-coil control in distribution systems. IEEE Transactions on Industrial Electronics **57**(4), 1445–1451 (2010)
8. Ze, Z.: FASD based on BSC method for distribution networks. IET Generation **24**(13), 5487–5494 (2019)
9. Wang, W.: Principle and control design of active ground-fault arc suppression device for full compensation of ground current. IEEE Transactions on Industrial Electronics **64**(6), 4561–4570 (2017)
10. Chen, K.: Terminal open circuit voltage controller for Arc suppression in distribution network. IET Generation Transmission & Distribution **14**(3) (2020)